

# On the physical integrity of potential intensity theory

Michael T. Montgomery<sup>a1</sup> and Roger K. Smith<sup>b</sup>

<sup>a</sup> Dept. of Meteorology, Naval Postgraduate School, Monterey, CA, USA

<sup>b</sup> Meteorological Institute, Ludwig-Maximilians University of Munich, Germany

## Abstract:

Emanuel's potential intensity theory is widely accepted as providing a useful upper bound in tropical cyclone intensity theory for both forecasting and climate assessment purposes. However, recent revised observational and laboratory estimates of the mean value for the enthalpy and momentum exchange coefficients at near-surface wind speeds in major hurricanes have reduced the ratio of these coefficients to such an extent that potential intensity estimates, which depend on this ratio, are significantly reduced. In view of evidence that such estimates are already up to two intensity categories too low, a re-appraisal of the theory is called for. Such is the purpose of this paper. We have identified a range of issues with the theory that call into question its physical integrity. Some of the issues include the lack of a rotational constraint on the predicted intensity, its silence on the radial distance that air parcels are drawn inwards above the boundary layer, as well as its lack of dependence on the gravitational acceleration of the planet. The most major issue is that the assumed flow configuration of the theory is not dynamically consistent with the assumption of a steady state flow and could not emerge from any physically realistic initial-value problem. Some implications of these findings are discussed.

KEY WORDS Tropical cyclones, typhoons, hurricanes, potential intensity

Date: January 7, 2026; Revised ; Accepted

## 1 Introduction

2 Late last century saw much theoretical work focused  
3 on estimating the maximum potential intensity that a  
4 tropical cyclone can achieve in a particular environment  
5 (Emanuel 1986, 1988, 1995; Holland 1997; Bister and  
6 Emanuel 1998). An appraisal of these theories and a list  
7 of references is given by Camp and Montgomery (2001),  
8 who concluded that Emanuel's theory comes closest to  
9 providing a useful calculation of maximum intensity.  
10 However they noted also several shortcomings in the  
11 theory, arguing the need for more basic research on the  
12 axisymmetric and asymmetric dynamics of hurricanes.

13 Two years later, intensive observational data col-  
14 lected during category-five Hurricane Isabel (2003)  
15 over a three day period, and analyzed in the con-  
16 text of Emanuel's potential intensity (hereafter PI) the-  
17 ory, demonstrated shortcomings in the PI predictions  
18 by roughly two hurricane intensity categories over this  
19 period (Bell and Montgomery 2008). This discrepancy  
20 turns out to be quite conservative given recent revised  
21 observational and laboratory estimates of the mean value  
22 for the enthalpy and momentum exchange coefficients at  
23 near-surface wind speeds in major hurricanes (Smith and  
24 Montgomery 2023, Chapter 7, Section 2 below). These  
25 observational and laboratory observations give a reduced  
26 value for the mean ratio of these exchange coefficients,

27 which is a key parameter in PI theory, by a factor of  
28 approximately 70% compared with the base value used  
29 in Bell and Montgomery (2008).

30 In addition to these observational advances, there  
31 have been advances in our understanding of other ele-  
32 ments of the hurricane heat engine model. One such  
33 line of research has re-examined the basis of prior work  
34 incorporating dissipative heating in the PI theory. Speci-  
35 cally, Zhang (2010) and Kieu (2015) found that Bister  
36 and Emanuel (1998) overestimated the influence of dis-  
37 sipative heating in the tropical cyclone boundary layer.  
38 Kieu pointed also to an inconsistency of the Bister and  
39 Emanuel formulation and recommended use of the origi-  
40 nal PI formulation of Emanuel (1986), which neglects the  
41 effect of dissipative heating. Another line of research has  
42 examined more deeply the consequences of irreversible  
43 processes in the hurricane system. Specifically, Pauluis  
44 and Zhang (2017) investigated the impact of irreversible  
45 processes associated with precipitation and evaporation  
46 on the mechanical efficiency of deep eyewall convection  
47 and outer rainbands. Using idealized, three-dimensional,  
48 cloud-representing simulations of hurricanes, they found  
49 that the mechanical efficiency of deep convection in the  
50 hurricane eyewall, while significantly higher than that of  
51 the outer rainbands, is nonetheless reduced to approx-  
52 imately 70 % of its idealistic value in the equivalent  
53 Carnot-like heat engine model. The latter work implies  
54 that the mechanical efficiency factor employed in the PI  
55 model should be reduced by 30% .

56 In the light of the foregoing developments, it seems

<sup>1</sup>Correspondence to: Prof. Michael T. Montgomery, Dept. of Meteorology, Naval Postgraduate School, Monterey, CA, USA. E-mail: mtmontgo@nps.edu

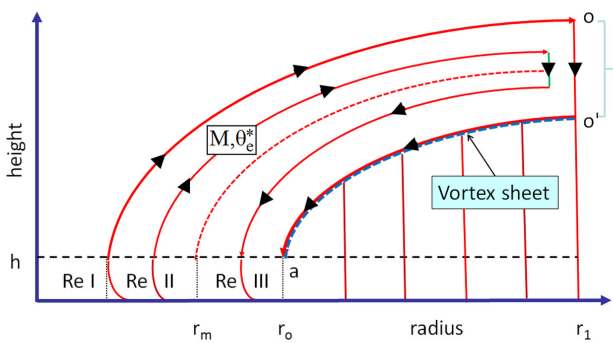


Figure 1. Schematic diagram of Emanuel's 1986 model for a steady-state mature hurricane. The arrows indicate the direction of the overturning circulation. The radial extent of the regions I-III are not drawn to scale. Typically, Region III is radially much more extensive than the others. See text for discussion. Adapted from [Montgomery and Smith \(2017\)](#).

appropriate to revisit earlier PI calculations and re-examine more deeply the fundamental basis for PI theory and its principal dependencies. This is particularly the case because of the widespread acceptance of PI theory over a period of four decades and its many applications to climate assessments (e.g., [Camargo et al. 2014](#), [Sobel et al. 2019](#), [Kieu et al. 2025](#)).

Over the years, the [Emanuel \(1986\)](#) paper (henceforth E86) has had a major influence within the tropical cyclone community and forms the basis of theoretical treatments of tropical cyclone structure in prominent text books ([Holton 2004](#), [Holton and Hakim 2013](#), [Houze 1993, 2014](#)). It led also to theories for tropical cyclone intensification. The intensification theories are examined in recent studies by [Montgomery and Smith \(2022\)](#), [Smith et al. \(2025\)](#) and [Smith and Montgomery \(2025\)](#), where a list of references may be found. One finding emerging from these studies is that, as a result of the assumed congruence and other assumptions, the axisymmetric, steady-state model configuration on which PI theory is based cannot be achieved in an Eliassen balance initial-value problem framework in which moist neutrality is used as a parameterization of moist convection. This is a further reason to question the integrity of PI theory, itself, which is the purpose of the current paper.

## 2 PI theory in brief

A comprehensive description of Emanuel's PI theory including many detailed derivations is given in [Smith and Montgomery \(2023\)](#), Chapter 13, and it suffices here to provide just a brief review of the main features and assumptions. The assumed flow configuration is shown in Fig. 1. The theory assumes hydrostatic balance and gradient wind balance above the boundary layer and

uses a quasi-linear slab boundary model in which departures from gradient wind balance are assumed negligibly small<sup>1</sup>. The boundary layer is taken to have constant depth,  $h$ , in which the absolute angular momentum,  $M$ , and pseudo-equivalent potential temperature,  $\theta_e$ , are well mixed at leading order. This layer is divided into three regions as shown in the figure: the eye region (Re I), the eyewall region (Re II) and the region beyond the eyewall (Re III). Region III is where spiral rainbands and shallow convection are assumed to operate in the vortex above (not depicted).

The quantities  $M$  and  $\theta_e$  are assumed to be materially conserved after an air parcel leaves the boundary layer and immediately ascends in the eyewall cloud. The ascending moist air parcels are assumed to rise slantwise through the troposphere, detrain at or near the tropopause level and then move to outer radii. In the steady model, the parcel trajectories and streamlines of the secondary (overturning) circulation are equivalent. Since the flow is assumed steady and  $M$  and  $\theta_e$  are materially conserved above the boundary layer, the  $M$  and  $\theta_e$  surfaces must be congruent there. The precise values of  $M$  and  $\theta_e$  at a particular radius are determined by the frictional boundary layer.

The model assumes that the radius of maximum tangential wind speed,  $r_m$ , is located at the outer edge of the eyewall cloud (outer edge of Re II in Fig. 1), although observations clearly indicate that  $r_m$  is closer to the inner edge ([Marks et al. 2008](#), Fig. 3). The middle dashed curve emanating from  $r_m$  is the  $M$ -surface along which the vertical velocity is zero and demarcates the region of ascent in the eyewall from that of large-scale descent outside the eyewall. The gradient wind at the top of and within the boundary layer is assumed to vanish at  $r_o$ . The entire flow beyond  $r_o$  and below the  $M$  surface passing through  $r_o$  is assumed to be quiescent. This outer dashed curve indicates the location of a vortex sheet as described in [Smith et al. \(2014\)](#).

The flow segment between  $o$  and  $o'$  in the upper right corner of the figure at radius  $r_I$  ( $r_I > r_o$ ) represents the assumed isothermal leg noted below and is the location at which air parcels are assumed to steadily gain cyclonic relative angular momentum ( $rv$ ) from the environment. This gain of angular momentum is needed in order to replace the frictional loss at the surface where the flow is cyclonic and is necessary for a steady state to exist. However, it is pertinent to inquire whether this source is physically plausible? For the moment, we will set aside this issue and focus on the presumed steady solution.

The energetics of the PI model are often likened to that of a Carnot cycle in which the inflowing air in the boundary layer acquires sensible and latent heat

<sup>1</sup>If the departures from gradient wind balance are assumed to be negligibly small and if the well-mixed boundary layer is to be continuous with the gradient wind at the boundary layer top, it follows logically that the tangential flow in the boundary layer must be in gradient wind balance at leading order.

(principally latent heat) while remaining approximately isothermal. The ascending air is assumed to be pseudo-moist adiabatic<sup>2</sup> and the outflowing air at large radius is assumed to descend isothermally in the upper atmosphere. This isothermal subsidence would require the accompanying adiabatic compression to be exactly balanced by radiative cooling to space. The final leg in the cycle is assumed to follow a reversible moist adiabat. *This leg is arguably the most implausible since for one thing, the time scale required for air parcels to descend back to the sea surface is on the order of one month, far longer than the typical life cycle of an individual hurricane.* A further issue is that, in clear sky conditions, the radiative cooling acts throughout the troposphere. Thus,  $\theta_e$  cannot be materially conserved in the descending leg. Bister et al. (2011) have pointed out, *inter alia*, that this hypothetical dissipative heat engine does no useful work on its environment.

The main outcome of the PI formulation is a closed expression for the maximum gradient wind at the top of the boundary layer  $v_{gmax}$ . The solution for  $v_{gmax}^2$  is found to be approximated by<sup>3</sup>:

$$v_{gmax}^2 = \frac{C_K}{C_D} \epsilon L_v r_{va}^* (1 - RH_{as}) \times \frac{1 - \frac{f^2 r_o^2}{4\beta R_d T_B}}{1 - \frac{\epsilon L_v r_{va}^* (1 - RH_{as}) C_K}{2\beta R_d T_s C_D}}, \quad (1)$$

where  $L_v$  is the latent heat of condensation of water vapour,  $R_d$  is the specific gas constant for dry air,  $T_s$  is the sea surface temperature,  $\epsilon = (T_B - T_0)/T_B$  is the thermodynamic efficiency factor,  $T_B$  is the averaged temperature of the boundary layer (assumed constant with radius),  $T_0$  is the average outflow temperature weighted with the saturated moist entropy of the outflow angular momentum surfaces (Eq. (19) of Emanuel 1986)<sup>4</sup>,  $r_{va}^*$  is the saturation mixing ratio at the top of the surface layer in the environment,  $RH_{as}$  is the ambient relative humidity at the top of the surface layer,  $\beta = 1 - \epsilon(1 + L_v r_{va}^* RH_{as} / R_d T_s)$  and  $r_o$  is the radial extent of the storm near sea level (nominally the radius at which  $v = 0$ )<sup>5</sup>.

By the early 2000s, the E86 theory was considered useful to the community because it offered a relatively simple framework for estimating a storm's maximum intensity that is well within an order of magnitude of

observations. The theory has been used widely to estimate the impact of global climate change on tropical cyclone intensity and structure change. As an illustration of its influence, the E86 formulation continues to be used as a foundation for revising the steady-state theory (e.g., Garner 2015) as well as for estimating the impact of global warming scenarios on tropical cyclone intensity and structure (Emanuel 1988; Camargo et al. 2014; Sobel et al. 2019; Kieu et al. 2025).

From Eq. (1), Emanuel constructed curves for  $v_{gmax}$  as a function of upper-level outflow temperature and sea surface temperature. As an example, for a sea surface temperature of 28°C and an outflow temperature of -60°C, the formula predicts a  $v_{gmax}$  of approximately 60 m s<sup>-1</sup> (see Fig. 2a). In this calculation, it is assumed that  $C_K/C_D = 1$ , but the latest field observations and laboratory measurements synthesized in Bell et al. (2012) and Curcic and Haus (2020) suggest a mean value of approximately  $C_K/C_D \approx 0.32$  in the high wind speed range (Smith and Montgomery 2023). Although Bell et al. (2012) acknowledge the scatter in the observational estimates of  $C_K/C_D$  in the high wind speed regime (see Chapter 13 of Smith and Montgomery 2023, where the recent findings of Curcic and Haus 2020 are discussed also), these data still represent our best mean estimates at the time of writing<sup>6</sup>. For such a reduced ratio of mean exchange coefficients, and for the selected temperatures, Eq. (1) predicts a reduced  $v_{gmax}$  of approximately 34 m s<sup>-1</sup> (see Fig. 2b), a minimal hurricane with an intensity significantly less than that obtained using  $C_K/C_D = 1$ <sup>7</sup>.

### 3 A few basics on tropical cyclone dynamics

As a prelude to understanding the issues we have with PI theory, it seems worthwhile to revisit a few basic features of vortex intensification in general. In a recent summary of the processes that operate during the tropical cyclone life cycle, Smith and Montgomery (2025) noted two important requirements for vortex intensification: a source of rotation and a mechanism to concentrate that rotation. The interplay between these processes can be illustrated by a simple laboratory experiment reported by Turner and Lilly (1963): see Section 2.2 of Smith and Montgomery. In this experiment, which was originally intended to illustrate how a tornado vortex can develop downwards from a rotating thunderstorm, the forcing was

<sup>2</sup>Contrary to statements made in E86, the formulation assumes pseudo-adiabatic rather than reversible thermodynamics in which all condensate rains out instantaneously (Bryan and Rotunno 2009, p3044). It is not a true Carnot cycle, in part, because of the irreversible nature of the precipitation process in the eyewall region of the vortex (also Pauluis and Zhang 2017).

<sup>3</sup>Eq. (43) of Emanuel (1986)

<sup>4</sup>This is the temperature at which air parcels are assumed to descend approximately isothermally in the upper atmosphere.

<sup>5</sup>The mathematical definition for  $r_o$  is given by Eq. (20) of Emanuel (1986).

<sup>6</sup>For simplicity, the intensity estimates summarized herein neglect dissipative heating and do not include the reduction of mechanical efficiency as discussed in the Introduction.

<sup>7</sup>If one generalizes the axisymmetric E86 formulation to estimate the impact of vertical shear of the environmental wind (e.g., Tang and Emanuel 2010) and turbulent ocean mixing in the wake of a moving storm (e.g., Miyamoto et al. 2017), the latter estimate is reduced still further. Including the 30% reduction in mechanical efficiency found by Pauluis and Zhang (2017) reduces the gradient wind intensity estimate even more.

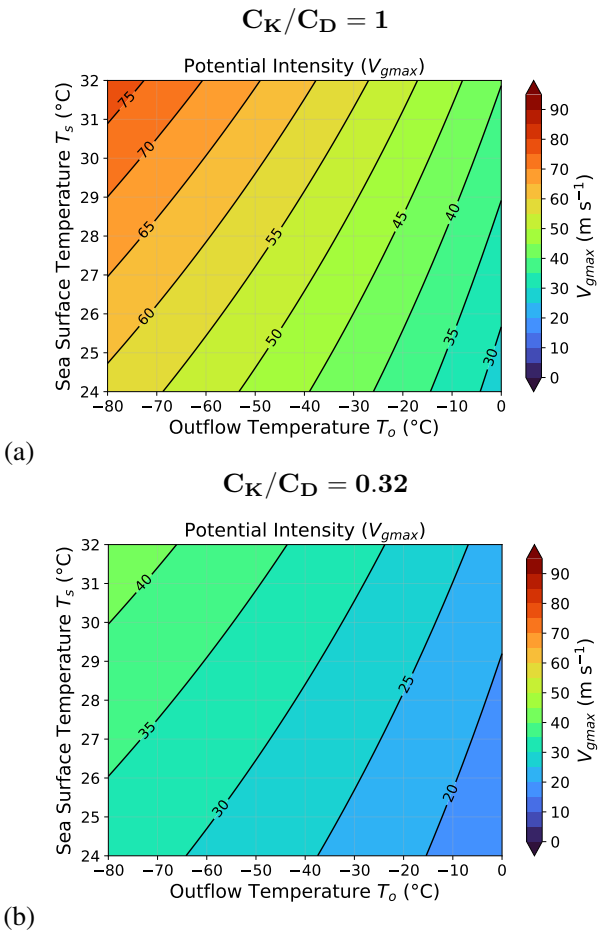


Figure 2. Predicted  $v_{g\max}$  curves in  $\text{m s}^{-1}$  from Eq. (1) as a function of sea surface temperature ( $T_s$ ) and outflow temperature ( $T_o$ ) from Emanuel's 1986 model for a mature steady-state hurricane. Temperature is in Celsius. The ratio of moist entropy to momentum transfer coefficients  $C_K/C_D$  is assumed here to be unity. Calculations assume also an ambient surface pressure of 1015 mb, an ambient near-surface relative humidity (RH) of 80%, a Coriolis parameter  $f$  evaluated at 20 degrees latitude, and an outer radius  $r_o$  equal to 500 km. See text for further details. Adapted from Emanuel (1986).

When the downwards-growing vortex begins to frictionally interact with the lower boundary of the cylinder, rings of water no longer conserve their absolute angular momentum and a boundary layer forms near the surface. This boundary layer reduces the rotational constraint on inflow and will have an influence on the final steady-state vortex through its constraint on the meridional (overturning) circulation forced by the bubbles.

Smith and Montgomery (2025) suggested that the dynamical constraints illustrated by the Turner-Lilly experiment should apply also to tropical cyclones. In fact, the modifications required in such an application were explored more than a decade ago by Smith et al. (2011) using a simple three-layer tropical cyclone model. As in the laboratory experiments, the latter study found that the strongest vortices, as characterized by their final wind intensity, develop in environments with intermediate background rotation (Fig. 3). However, in the tropical cyclone case, one cannot separately control the forcing strength and the rotation strength. A related line of inquiry examining the dependence of vortex intensity on the initial vortex size is summarized in Section 16.5 of Smith and Montgomery (2023), albeit in the context of a more sophisticated, three-dimensional numerical model. At this point, the question arises whether PI theory shows a similar behaviour and, if not, why not? We address these questions below.

## 4 Appraisal of PI theory

### 4.1 A puzzling feature and some questions

As noted by Smith and Montgomery (2023), a puzzling feature of the E86 derivation is that there seems to be no mathematical constraint on the gradient wind,  $v_g$  whereby  $\partial v_g / \partial r = 0$  at the radius,  $r_{\max}$ , where  $v_g$  is a maximum. In fact, all derivations using the E86 formalism appear not to predict the location of  $r_{\max}$ , at least in terms of *a priori* known quantities, e.g., the radius of initial maximum tangential wind, the initial relative vorticity distribution or the ambient planetary vorticity. However, the ability to predict a storm's minimum inner-core size given knowledge of its incipient structure is a central problem in tropical cyclone dynamics and forecasting since, as intimated in Section 3, the inner-core size is related to how far air parcels are drawn inwards above the friction layer by the aggregate deep convection in the core region of the vortex.

As an example, in a simple axisymmetric configuration, if a ring of air rotating at a speed of  $5 \text{ m s}^{-1}$  at a radius of 200 km is drawn inwards above the boundary layer to a radius of 20 km while conserving  $M$ , its tangential velocity will be  $50 \text{ m s}^{-1}$  at the Equator ( $f = 0$ ), whereas at a latitude of 10 degrees, the velocity would be  $75 \text{ m s}^{-1}$  and at 15 degrees it would be  $87 \text{ m s}^{-1}$ . Even starting with zero initial tangential velocity,

modelled by a source of air bubbles from an elevated tube positioned along the axis of a cylindrical tank of water in solid body rotation. The bubbles have an effect analogous to cloud buoyancy in a tornadic thunderstorm.

Interpretations of vortex development in the Turner-Lilly experiment were eloquently articulated by Morton (1966). For a given rotation rate of the tank, the formation of a concentrated vortex core requires an optimum forcing strength as characterized by the bubbling rate of air. Vortex intensity depends on how far rings of water can be drawn inwards above the boundary layer while conserving their absolute angular momentum. This distance depends on the strength of the mechanism drawing rings inwards, i.e., the bubbling rate, and on the rotational constraint imposed by the tangential wind distribution, which inhibits the inwards displacement.

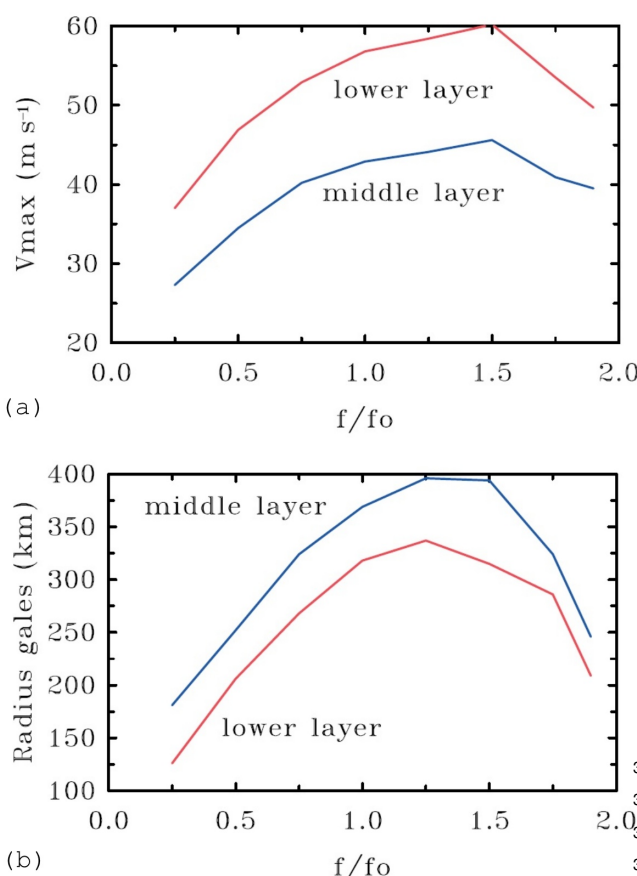


Figure 3. Variation of (a) the maximum tangential wind, and (b) radius of gales (based on this wind component) with the Coriolis parameter in the lower and middle layers of a three-layer, axisymmetric, tropical cyclone model at 12 days in the calculations described in Section 4 of Smith et al. (2011). The reference value of the Coriolis parameter,  $f_0$ , corresponds to a latitude of 20°.

the same radial displacement at a latitude of 15 degrees would give a tangential velocity of 37 m s<sup>-1</sup>. Clearly, the radial displacement has to be important in the determination of  $v_{gmax}$  and this displacement must depend on the forcing mechanism driving inflow.

The foregoing back-of-the-envelope calculation leads to a dilemma in understanding PI theory. First, the assumed flow configuration in that theory has outflow everywhere above the boundary layer and *the assumption that ascending flow is moist neutral there means that there is no local buoyancy analogous to the forcing by bubbles in the Turner-Lilly experiment*. However, it is clear from the foregoing discussion that, without a knowledge of radial displacements of air parcels above the boundary layer as well as the mechanism forcing these displacements, a steady-state theory assuming outflow everywhere above the boundary layer must be viewed with utmost caution. This caution is partly because a knowledge of the radial displacement of air parcels can be achieved only by solving a time-dependent initial-value

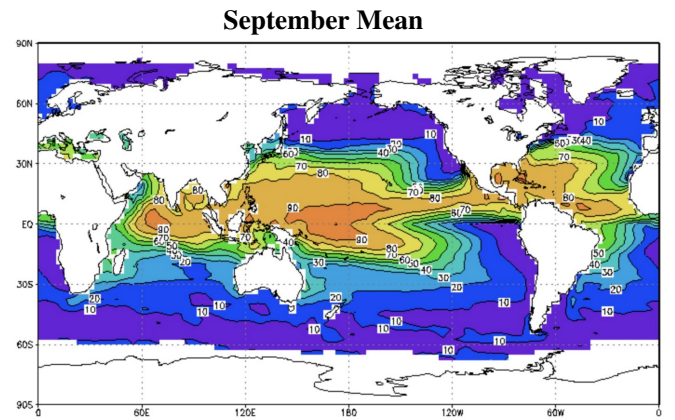


Figure 4. Example of hurricane monthly global PI map for surface wind speed for September in m s<sup>-1</sup>. The calculations assume  $C_K/C_D = 1$ , include dissipative heating and use the reversible Carnot efficiency as discussed in the Introduction. The calculations use the National Centers for Environmental Prediction re-analysis data during the years 1982-1995, inclusive, and Reynolds' CAC Global Sea Surface optimum interpolation temperature analysis. Courtesy of M. Bister and MIT (<https://wind.mit.edu/~emanuel/pcmin/climo.html>).

problem in which the forcing of the overturning circulation is accounted for. It is also because of the well known fact that, without any forcing to oppose the overturning circulation driven by friction alone, the flow will spin down (Greenspan and Howard 1963; see also Section 2.2.2 of Smith and Montgomery 2025). We return to these questions in Section 4.6.

## 4.2 Ambient rotation issues

Based on the considerations outlined in Section 3, a key feature of tropical cyclone behaviour is the expected control on the flow structure imposed by the ambient planetary vorticity (i.e., the ambient Coriolis parameter,  $f$ , assumed constant in this discussion for simplicity). It is well known that a tropical cyclone will not exist without ambient rotation to concentrate (see, e.g., Smith and Montgomery 2023, Section 2.16). However, Eq. (1) predicts only a weak dependence of the PI on the ambient Coriolis parameter. Specifically, the only term in Eq. (1) involving  $f$  is the non-dimensional term in the numerator ( $f^2 r_0^2 / 4\beta R_d T_B$ ), which is subtracted from unity. This term is associated with the energy required to spin up the outer anticyclone in the upper troposphere. It acts to reduce the maximum tangential velocity, but is generally small using typical parameters ( $O(3 \times 10^{-3}) \ll 1$ ). Hence, setting  $f$  to zero gives virtually identical predictions for  $v_{gmax}$  with a virtually identical dependence on outflow temperature and sea surface temperature as depicted in Fig 2.

Global maps of PI using Eq. (1) displayed over the tropics generally predict the strongest intensity along the equator where the planetary vorticity is identically zero

346 and the sea surface temperatures are the warmest (see, 397  
 347 e.g., Fig. 4). However, a maximum PI along the equator 398  
 348 is clearly incorrect since an intense cyclonic mesoscale 399  
 349 vortex cannot form in an environment with zero vertical 400  
 350 vorticity! The upshot is that a correct PI theory should 401  
 351 reflect the near-dearth of tropical cyclones along the 402  
 352 equator in the corresponding PI maps. 403  
 404  
 405

### 353 4.3 The silence on the gravitational acceleration 406 354

355 The PI formula given by Eq. (1) is not dependent on 408  
 356 the gravitational acceleration of the Earth. This means 409  
 357 that the predicted maximum gradient wind will be the 410  
 358 same if one were to hypothetically halve or double the 411  
 359 gravitational acceleration! The reason for this silence is 412  
 360 presumably because of the assumption of moist neutral 413  
 361 ascent above the boundary layer. This assumption implies 414  
 362 that there is no local buoyancy forcing of the overturning 415  
 363 circulation above the boundary other than that produced 416  
 364 by the frictional boundary layer, itself (see Section 4.6). 417  
 418  
 419

### 365 4.4 Boundary layer issues

366 Another key feature of tropical cyclone behaviour is the 419  
 367 control on the flow structure exerted by the frictional 420  
 368 boundary layer. This control leads to subtle changes in 421  
 369 storm structure during the tropical cyclone life cycle 422  
 370 (Smith et al. 2015; Kilroy et al. 2015, Section 4; Smith 423  
 371 et al. 2021). Various aspects of the boundary layer with 424  
 372 implications for PI theory are discussed below. 425  
 426  
 427

#### 373 4.4.1 Boundary layer wind speed enhancement

374 Basic studies of the nonlinear boundary layer of a trop- 429  
 375 ical cyclone using a simple axisymmetric slab model 430  
 376 revealed a property whereby, in general, the maximum 431  
 377 tangential wind speed in the boundary layer exceeds that 432  
 378 at the boundary layer top (Smith and Vogl 2008). The 433  
 379 consequences of this result in relation to PI theory were 434  
 380 explored by Smith et al. (2008), who pointed out, *inter* 435  
 381 *alia*, that it is not possible to incorporate this effect into 436  
 382 PI theory. As noted in Section 2, PI theory is based on 437  
 383 the assumption of balance dynamics everywhere, includ- 438  
 384 ing the boundary layer at leading order. This formulation 439  
 385 requires that angular momentum exiting the well-mixed 440  
 386 boundary layer equals that at the boundary layer top with- 441  
 387 out the need for adjustment to gradient wind balance. 442  
 388  
 389

390 The existence of the maximum tangential wind in 443  
 391 the boundary layer has been well documented in both 444  
 392 three-dimensional numerical model simulations of tropi- 445  
 393 cal cyclones (e.g., Zhang et al. 2001; Smith and Thomsen 446  
 394 2010) as well as in observations studies of these storms 447  
 395 (Bell and Montgomery 2008; Nolan et al. 2009a,b; Mont- 448  
 396 gomery et al. 2014; Sanger et al. 2014; Smith et al. 449  
 397 2018a). The mechanism by which the tangential wind 450  
 398 maximum develops in the boundary layer rather than 451  
 399

400 above is a particular feature of vortex boundary layers 401  
 402 and is now known as *the nonlinear boundary layer spin- 403  
 404 up enhancement mechanism* (see Smith and Montgomery 405  
 406 2023, Section 6.6).

407 The role of this boundary layer spin up enhancement 408  
 409 mechanism in determining the maximum tangential wind 410  
 411 was shrugged off by Emanuel and Rotunno (2011), who 412  
 413 suggested that nonlinear boundary layer effects were 414  
 415 generally neutralized in regards to their influence on the 416  
 417 maximum gradient wind at the top of the boundary layer, 418  
 419 as well as its location (see next subsection).

#### 4.4.2 Boundary layer dependence on the gradient wind profile

420 It has been long recognized that the radial profiles of 421  
 422 horizontal wind components in the boundary layer as well 423  
 424 as the vertical velocity at the boundary layer top have a 425  
 425 significant dependence on the radial profile of gradient 426  
 427 wind. This dependence is highlighted by some recent 428  
 428 steady, axisymmetric, slab boundary layer calculations of 429  
 430 Smith and Montgomery (2026), summarized in Fig. 4. 431  
 431 This figure shows results for six gradient wind profiles 432  
 432 with the same maximum gradient wind,  $40 \text{ m s}^{-1}$  and 433  
 433 the same radius at which it occurs,  $40 \text{ km}$  (panel (a)), but 434  
 434 with different outer widths. The remaining panels in the 435  
 435 figure show the radial and tangential wind speeds in the 436  
 436 boundary layer as well as the vertical velocity at the top 437  
 437 of the boundary layer for each gradient wind profile.

438 For relatively narrow outer wind profiles, the 439  
 440 tangential wind can significantly exceed the gradient wind 441  
 442 maximum and this maximum can occur well inside the 443  
 443 radius of maximum gradient wind. Both of these 444  
 444 features have been confirmed observationally using high- 445  
 445 resolution dropwindsonde deployments in conjunction 446  
 446 with aircraft reconnaissance data and airborne dual- 447  
 447 Doppler radar analyses for intensifying tropical cyclones 448  
 448 (e.g., Montgomery et al. 2014; Sanger et al. 2014). In 449  
 449 contrast, for broader outer wind profiles, the tangential 450  
 450 wind maximum is only modestly greater than the gradient 451  
 451 wind maximum and the radial location of this maximum 452  
 452 progressively moves outward beyond the initial gradient 453  
 453 wind maximum. These broad wind profile experiments 454  
 454 illustrate an intrinsic tendency for broad wind fields to 455  
 455 develop a secondary tangential wind maximum exterior 456  
 456 to the initial gradient wind maximum. These experiments 457  
 457 offer a simple explanation as to why maturing tropical 458  
 458 cyclones, which typically grow in size with time, are 459  
 459 prone to forming secondary eyewalls (e.g. Huang et al. 460  
 460 2018 and refs.) even in the absence of adverse environmental 461  
 461 factors that might disrupt the inner-core convection, e.g. vertical shear.

462 These results have major consequences for PI theory 463  
 463 since the PI formula given by Eq. (1) above has no 464  
 464 dependence on the outer wind profile. This silence is 465  
 465 surprising in view of the dynamical processes operating in 466  
 466 the boundary layer as air parcels approach the inner core 467  
 467

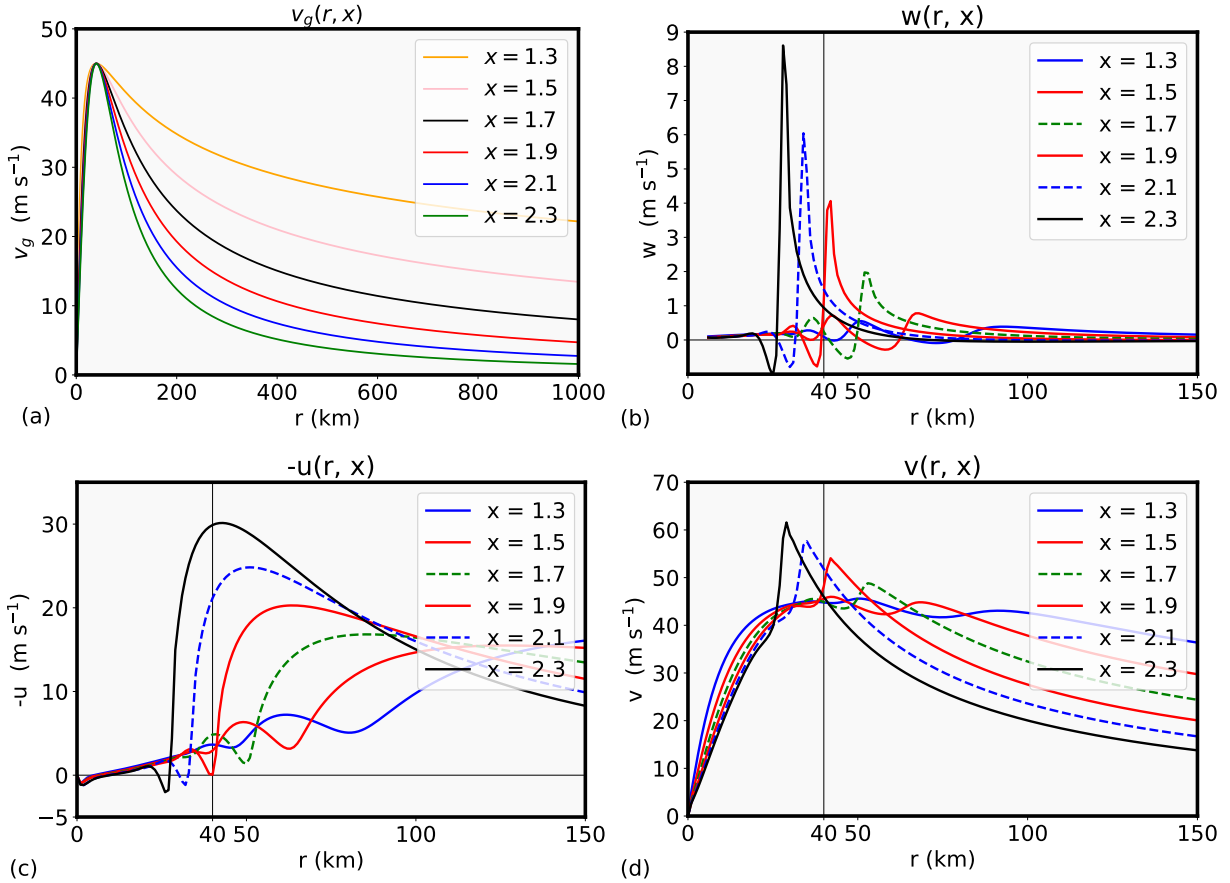


Figure 5. Radial profiles of: (a) gradient wind out to 1000 km; (b) vertical velocity at the boundary layer top; and (c), (d) radial and tangential velocity components in the boundary layer, respectively, at radii inside 150 km in the nonlinear solutions obtained using Method 1 for the six gradient wind profiles in (a). The radial velocities in (c) are plotted with positive values representing inflow and negative values outflow. The location of the radius of maximum gradient wind at 40 km is highlighted in panels (b)-(d) by a thin vertical line. Adapted from [Smith and Montgomery \(2026\)](#).

region. In contrast, the slab boundary layer calculations of [Smith and Montgomery](#) point to an important role of the outer wind structure in determining the maximum system-scale tangential and radial wind of the boundary layer. In particular, they demonstrate the importance of boundary-layer dynamics outside the radius of maximum gradient wind in determining (i) where the air erupts out of the boundary layer and (ii) how strong the tangential wind and radial wind can become as air parcels move inwards towards the centre of circulation. These features are encapsulated in the idea of boundary layer control ([Smith and Montgomery 2023](#)).

It is worth noting that because the tangential wind at the top of Region III (see Fig. 1) is obtained from thermodynamic considerations in the boundary layer, in conjunction with the assumptions of thermal wind balance and congruity of  $M$  and reversible saturation equivalent potential temperature ( $\theta_e^*$ ) surfaces above the boundary layer, the dynamics of the boundary layer in Region III have been ignored completely. The foregoing results show that these assumptions are significant limitations of the PI model.

#### 4.4.3 Horizontal diffusion in the boundary layer

In the context of Emanuel's PI theory and its extension to account for unbalanced effects at and above the boundary layer top by [Bryan and Rotunno \(2009\)](#), [Smith and Montgomery \(2026\)](#) provided an assessment of a conjecture made by Bryan and Rotunno in subsequent research in regards to the practical usefulness of the E86 model (and subsequent variants - see [Smith and Montgomery 2023](#), Chapter 13, for a detailed summary) and its key intensity prediction by way of Eq. (1). In the E86 formulation, a simplified form of the linearized slab boundary layer is employed that uses just the tangential component of the slab Ekman layer, assumes the tangential velocity in the boundary layer is *equal to* the gradient wind at leading order, and neglects the lateral diffusion of absolute angular momentum.

[Rotunno and Bryan \(2012\)](#) conjectured that for practical purposes the E86 slab boundary layer model should serve as an adequate boundary layer closure for the maximum intensity problem, in part because the E86 slab model represents a compromise between offsetting effects involving nonlinear advective dynamics and the

radial diffusion of horizontal momentum in the boundary layer. However, in the nonlinear boundary calculations presented by Smith and Montgomery (2026), the solution of the equations with lateral diffusion retained *was virtually unaffected* by lateral diffusion. This fact is important since the lateral eddy momentum diffusion employed in the calculations was  $5,000 \text{ m}^2 \text{ s}^{-1}$ , notably larger than the average observed horizontal diffusivity in hurricanes possessing maximum wind speeds in the range of 40 to  $60 \text{ m s}^{-1}$  (Zhang and Montgomery 2012, their Fig. 6). The calculations offer a quantitative rebuttal to the conjecture, at least within the context of the slab boundary layer, that horizontal diffusion acts to significantly ameliorate the concentration of momentum and entropy in the boundary layer and the lofted values thereto in the vortex interior.

The reasoning behind this rebuttal is that, despite the presence of surface drag, the strong radial inflow in the boundary layer, driven by the nonlinear agradient force, acts efficiently to concentrate absolute angular momentum in the boundary layer. As is shown in Smith and Montgomery (2026), for narrow vortex profiles, this concentration has a propensity to produce shock-like structures inside the gradient wind maximum, not unlike the shock-like structure observed in the low-level wind structure of Hurricane Hugo (Marks et al. 2008) and recent high-resolution mesoscale hurricane simulations (Kuo et al. 2022). Horizontal diffusion would have to take on unrealistically large values to ameliorate this shock structure.

## 4.5 The existence of a steady state

The statement that a tropical cyclone is in a (quasi-) steady state can be misleading as this is usually based on the steadiness of the intensity: it does not mean that the entire flow is in any way steady globally. The requirements for a strict steady state are quite severe and are not likely to be even approximately attained, either in numerical models or in reality (Smith et al. 2014, Persing et al. 2019). In fact, in both numerical models and in reality, tropical cyclones undergo a life cycle of growth, maturity and decay (e.g., Smith et al. 2021, Vinour and Montgomery 2026). For one thing, a global steady state would require the existence of a steady supply of cyclonic relative angular momentum to replenish that lost on account of surface friction.

In PI theory, the cyclonic angular momentum lost by surface friction must be replenished at large radii in the upper troposphere (the path o-o' in Fig. 1), but the required amount is simply determined by the problem itself. It is not an externally specified quantity. Nevertheless, as pointed out in Section 4.1, elementary considerations indicate that the flow configuration in PI theory is one in which a vortex would ordinarily spin down. We examine this issue next.

## 4.6 The initial-value problem dilemma

In Section 4.1, we showed that the intensity of a balanced vortex as measured by the maximum gradient wind depends sensitively on how far air parcels are displaced radially inwards above the boundary layer and on the strength of the ambient rotation. We argued also that a knowledge of this displacement can be achieved only by solving a time-dependent initial-value problem in which the forcing of the overturning circulation is taken into account. However, because the flow above the boundary layer in PI theory is moist neutral, the only forcing mechanism for the overturning circulation is the frictional boundary layer, in which case the vortex would ordinarily spin down. This conclusion points to an inconsistency in PI theory, but where is this inconsistency?

A clue arises from the study by Smith et al. (2025), mentioned in the Introduction. These authors showed that the axisymmetric flow configuration that forms the basis for the PI calculation cannot be achieved in an Eliassen balance initial-value problem framework in which moist neutrality is assumed as a parameterization of moist convection. Smith et al. showed further that the vortex in this initial-value problem spins down. *We conclude that the inconsistency referred to above stems from the assumption of a steady-state flow configuration for PI theory that, in fact, based on elementary dynamical reasoning, cannot exist as a steady state. This flow configuration is essentially one for vortex spin down* (see e.g. Smith et al. 2018b, especially Fig. 9 and related discussion, Smith and Wang 2018). The fact is that the congruence between the streamlines and  $M$ -surfaces implicit in the steady-state would be immediately destroyed by the frictional spin down of the overturning circulation associated with a weakening of the tangential flow immediately above the boundary layer top. This weakening is a result of the material conservation of  $M$  above the boundary layer in the presence of radial outflow.

## 5 Summary

We have identified above a range of issues that, in our view, both individually and collectively, raise serious questions about the integrity of axisymmetric PI theory and thereby the usefulness of this theory in tropical cyclone forecasting and in applications to formulating climate assessments relating to tropical cyclones. Specifically, we have noted the following issues of detail:

- the dubious assumptions along the descending branch of the circulation and the required steady source of cyclonic angular momentum (Section 2);
- the inaccuracy of the theory in the light of the revised mean estimates for the ratio of  $C_K/C_D$  (Section 2);

- the lack of a rotational constraint leading to a maximum PI at the equator (Section 4.1);
- the lack of a prediction for the location of  $r_{max}$  where  $\partial v_g / \partial r$  vanishes (Sections 4.1, 4.6);
- the lack of dependence on the Earth's gravity (Section 4.3);
- the silence on the nonlinear boundary layer spin-up enhancement mechanism (Section 4.4.1);
- the lack of dependence of the boundary layer flow on the radial profile of gradient wind (Section 4.4);
- the inability to achieve the assumed balanced steady state from an initial-value problem (Section 4.6);
- the lack of any physical forcing mechanism to drive ascent above the boundary layer (Section 4.1);
- inward radial displacements of order 200 km above the boundary layer can easily explain intensification to very intense storms, but inclusion of these effects is fundamentally a time dependent problem (Section 4.6, see also Smith et al. 2011).

The most important issue with PI theory as it stands is the dynamical inconsistency that the assumed flow configuration cannot remain in a steady state, as presumed. Rather, the flow would decay as in the classical spin down problem for a rotating fluid. It follows that such a steady-state flow could not emerge from any physically realistic initial-value problem (Section 4.6).

## 6 Conclusions

We have sought to appraise Emanuel's potential intensity theory, which is widely accepted as providing a useful upper bound in tropical cyclone intensity theory for both forecasting and climate assessment purposes. In doing this, we have identified a range of issues with assumptions on which the theory is based, which we believe are severe enough to compromise the integrity of the theory. Of these, the issue that stands out is the simple fact that the assumed flow configuration of the theory is not dynamically consistent with the presumption that the flow exists in a steady state. Indeed, we argue that this steady-state flow configuration could not materialize in any physically realistic initial-value problem. In fact, if imposed initially, the flow would begin immediately to spin down.

We anticipate that critics of our appraisal will argue that we have not yet produced an alternative theory, but

we have argued that any such theory must be fundamentally time dependent. This is because it needs to take into account how far air parcels can be drawn inwards above the boundary layer as well as the mechanism for producing this displacement. We acknowledge that the simplicity of the current PI formula or its variants will probably ensure their survival, at least until users begin to question the physics they embody. Despite this possibility, we would be remiss in not attempting to articulate the limitations of the theory as we see them for the tropical cyclone community. Indeed, for the reasons identified herein, we, at least, would be most uncomfortable in using current PI theory for any serious climate assessments.

## 7 Acknowledgements

We thank the National Science Foundation and MIT for making available the global PI maps used in Section 4.2 (<https://wind.mit.edu/~emanuel/pcmin/climo.html>). The views expressed herein are those of the authors and not of their corresponding institutions or funding agencies. MTM wishes to thank Timothy Dunkerton, James McWilliams and Joe Biello for their ongoing encouragement to pursue deeper understanding of severe tropical weather phenomena.

## References

Bell, M. M., and M. T. Montgomery, 2008: Observed structure, evolution, and potential intensity of Category 5 Hurricane Isabel (2003) from 12 to 14 September. *Mon. Wea. Rev.*, **136**, 2023–2046.

Bell, M. M., M. T. Montgomery, and K. A. Emanuel, 2012: Air-sea enthalpy and momentum exchange at major hurricane wind speeds observed during CBLAST. *J. Atmos. Sci.*, **69**, 3197–3222.

Bister, M., and K. A. Emanuel, 1998: Dissipative heating and hurricane intensity. *Meteor. Atmos. Phys.*, **50**, 233–240.

Bister, M., N. Renno, O. Paulius, and K. A. Emanuel, 2011: Comment on Makarieva et al. 'a critique of some modern applications of the carnot heat engine concept: the dissipative heat engine cannot exist'. *Proc. R. Soc. A*, **467**, 1–6, doi:10.1098/rspa.2010.0087.

Bryan, G. H., and R. Rotunno, 2009: Evaluation of an analytical model for the maximum intensity of tropical cyclones. *J. Atmos. Sci.*, **66**, 3042–3060.

Camargo, S. J., M. K. Tippett, A. H. Sobel, G. A. Vecchi, and M. Zhao, 2014: Testing the performance of tropical cyclone genesis indices in future climates using the HIRAM model. *J. Climate*, **27**, 9171–9196.

704 Camp, J. P., and M. T. Montgomery, 2001: Hurricane 752  
705 maximum intensity: Past and present. *Mon. Weather 753*  
706 *Rev.*, **129**, 1704–1717. 754  
707 Curcic, M., and B. K. Haus, 2020: Revised estimates 755  
708 of ocean surface drag in strong winds. *Geophysical 756*  
709 *Research Letters*, **47**, 1–8. 757  
710 Emanuel, K. A., 1986: An air-sea interaction theory for 758  
711 tropical cyclones. Part I: Steady state maintenance. *J. 759*  
712 *Atmos. Sci.*, **43**, 585–604. 760  
713 Emanuel, K. A., 1988: The maximum intensity of hurricanes. *J. Atmos. Sci.*, **45**, 1143–1155. 761  
714 Emanuel, K. A., 1995: Sensitivity of tropical cyclone to 762  
715 surface exchange coefficients and a revised steady-state 763  
716 model incorporating eye dynamics. *J. Atmos. Sci.*, **52**, 764  
717 3969–3976. 765  
718 Emanuel, K. A., and R. Rotunno, 2011: Self-stratification 766  
719 of tropical cyclone outflow. Part I: Implications for 767  
720 storm structure. *J. Atmos. Sci.*, **68**, 2236–2249. 768  
721 Garner, S., 2015: The relationship between hurricane 769  
722 potential intensity and CAPE. *J. Atmos. Sci.*, **72**, 141– 770  
723 163. 771  
724 Greenspan, H. P., and L. N. Howard, 1963: On a time- 772  
725 dependent motion of a rotating fluid. *J. Fluid Mech.*, 773  
726 **17**, 385–404. 774  
727 Holland, G. H., 1997: The maximum potential intensity 775  
728 of tropical cyclones. *J. Atmos. Sci.*, **54**, 2519–2541. 776  
729 Holton, J. R., 2004: *An Introduction to Dynamic Meteor- 777  
730 ology*, 4th Edition. Academic Press, London, 535pp. 778  
731 Holton, J. R., and G. Hakim, 2013: *An Introduction to 779  
732 Dynamic Meteorology*, 5th Edition. Elsevier, London, 780  
733 532pp. 781  
734 Houze, R. A., 1993: *Clouds dynamics*. Academic Press, 782  
735 San Diego, 570pp. 783  
736 Houze, R. A., 2014: *Clouds dynamics*, 2nd Edition. 784  
737 Academic Press, London, 496pp. 785  
738 Huang, Y.-H., C.-C. Wu, and M. T. Montgomery, 2018: 786  
739 Concentric eyewall formation in Typhoon Sinlaku 787  
740 (2008). Part III: Horizontal momentum budget analy- 788  
741 sis. *J. Atmos. Sci.*, **75**, 3541–3563. 789  
742 Kieu, C., 2015: Revisiting dissipative heating in tropical 790  
743 cyclone maximum potential intensity. *Quart. Journ. 791*  
744 *Roy. Meteor. Soc.*, **139**, 1255–1269, doi:10.1002/qj. 792  
745 2534. 793  
746 Kieu, C., S. Camargo, and H. Nguyen, 2025: Environ- 794  
747 mental controls on future projections of western North 795  
748 Pacific tropical cyclone maximum intensity. *npj Clim. 796*  
749 and *Atmos. Sci.*, **8**, 1–12, doi:[https://doi.org/10.1038/ 797](https://doi.org/10.1038/s41612-025-01214-6)  
750 800  
751 s41612-025-01214-6. 801  
752 Kilroy, G., R. K. Smith, and M. T. Montgomery, 2015: 753  
754 Why do model tropical cyclones grow progressively in 755  
756 size and decay in intensity after reaching maturity? *J. 757*  
757 *Atmos. Sci.*, **72**, 1783–1804.  
758 Kuo, H.-C., S. Tsujino, T.-Y. Hsu, M. S. Peng, and S.- 759  
759 H. Su., 2022: Scaling law for boundary layer inner 760  
760 eyewall pumping in concentric eyewalls. *J. Geophys. 761*  
761 *Research: Atmospheres*, **127**, 1–15, e2021JD035518. 762  
762 <https://doi.org/10.1029/2021JD035518>.  
763 Marks, F. D., P. G. Black, M. T. Montgomery, and R. W. 764  
764 Burpee, 2008: Structure of the eye and eyewall of 765  
765 Hurricane Hugo (1989). *Mon. Wea. Rev.*, **136**, 1237– 766  
766 1259.  
767 Miyamoto, Y., G. Bryan, and R. Rotunno, 2017: An 768  
768 analytical model of maximum potential intensity for 769  
769 tropical cyclones incorporating the effect of ocean 770  
770 mixing. *Geophys. Res. Letters.*, **44**, 5826–5835.  
771 Montgomery, M. T., and R. K. Smith, 2017: Recent 772  
772 developments in the fluid dynamics of tropical cyclones. 773  
773 *Annu. Rev. Fluid Mech.*, **49**, 541–574.  
774 Montgomery, M. T., and R. K. Smith, 2022: Minimal 775  
775 conceptual models for tropical cyclone intensification. 776  
776 *Tropical Cyclone Research and Review*, **11**, 61–75.  
777 Montgomery, M. T., J. A. Zhang, and R. K. Smith, 2014: 778  
778 An analysis of the observed low-level structure of 779  
779 rapidly intensifying and mature Hurricane Earl (2010). 780  
780 *Quart. Journ. Roy. Meteor. Soc.*, **140**, 2132–2146, 781  
781 doi:10.1002/qj.2283.  
782 Morton, B. R., 1966: *Geophysical vortices*, In *Prog. In 783  
783 Aeronautical Sci.*, Ed. Küchemann, Vol. 7. Pergamon, 784  
784 145–194 pp.  
785 Nolan, D. S., J. A. Zhang, and D. P. Stern, 2009a: Eval- 786  
786 uation of planetary boundary layer parameterizations 787  
787 in tropical cyclones by comparison of in situ obser- 788  
788 vations and high-resolution simulations of Hurricane 789  
789 Isabel (2003). Part I: Initialization, maximum winds, 790  
790 and the outer core boundary layer. *Mon. Wea. Rev.*, **137**, 791  
791 3651–3674.  
792 Nolan, D. S., J. A. Zhang, and D. P. Stern, 2009b: Eval- 793  
793 uation of planetary boundary layer parameterizations 794  
794 in tropical cyclones by comparison of in situ obser- 795  
795 vations and high-resolution simulations of Hurricane 796  
796 Isabel (2003). Part II: Inner core boundary layer and 797  
797 eyewall structure. *Mon. Wea. Rev.*, **137**, 3675–3698.  
798 Pauluis, O., and F. Zhang, 2017: Reconstruction of 799  
799 thermodynamic cycles in a high-resolution simulation 800  
800 of a hurricane. *J. Atmos. Sci.*, **74**, 3367–3381.  
801 Persing, J., M. T. Montgomery, R. K. Smith, and 802  
802 J. McWilliams, 2019: Quasi-steady hurricanes revis- 803  
803 ited. *Tropical Cyclone Research and Review*, **8**, 1–17.

802 Rotunno, R., and G. H. Bryan, 2012: Effects of param- 845  
803 eterized diffusion on simulated hurricanes. *J. Atmos. 846  
804 Sci.*, **69**, 2284–2299.

805 Sanger, N. T., M. T. Montgomery, R. K. Smith, and 849  
806 M. M. Bell, 2014: An observational study of tropical- 850  
807 cyclone spin-up in supertyphoon Jangmi from 24 to 27 851  
808 September. *Mon. Wea. Rev.*, **142**, 3–28.

809 Smith, R. K., G. Kilroy, and M. T. Montgomery, 2015: 852  
810 Why do model tropical cyclones intensify more rapidly 853  
811 at low latitudes? *J. Atmos. Sci.*, **72**, 1783–1804.

812 Smith, R. K., G. Kilroy, and M. T. Montgomery, 2021: 855  
813 Tropical cyclone life cycle in a three-dimensional 856  
814 numerical simulation. *Quart. Journ. Roy. Meteor. Soc.*, 857  
815 **147**, 3373–3393.

816 Smith, R. K., and M. T. Montgomery, 2023: *Tropical 859  
817 cyclones: Observations and basic processes*. Elsevier,  
818 London, 411pp.

819 Smith, R. K., and M. T. Montgomery, 2025: Towards 862  
820 understanding the tropical cyclone lifecycle. *Tropical 863  
821 Cyclone Research and Review*, **14**, 119–131.

822 Smith, R. K., and M. T. Montgomery, 2026: The axisym- 865  
823 metric slab boundary layer model underpinning the 866  
824 boundary layer control of tropical cyclones. *Tropical 867  
825 Cyclone Research and Review*, **15**, in press.

826 Smith, R. K., M. T. Montgomery, and S. A. Braun, 870  
827 2018a: Azimuthally-averaged structure of Hurricane 871  
828 Edouard (2014) just after peak intensity. *Quart. Journ. 872  
829 Roy. Meteor. Soc.*, **145**, 211–216.

830 Smith, R. K., M. T. Montgomery, and H. Bui, 2018b: 873  
831 Axisymmetric balance dynamics of tropical cyclone 874  
832 intensification and its breakdown revisited. *J. Atmos. 875  
833 Sci.*, **75**, 3169–3189.

834 Smith, R. K., M. T. Montgomery, and J. Persing, 2014: 878  
835 On steady-state tropical cyclones. *Quart. Journ. Roy. 879  
836 Meteor. Soc.*, **140**, 2638–2649, doi:10.1002/qj.2329.

837 Smith, R. K., M. T. Montgomery, and S. Vogl, 2008: A 880  
838 critique of Emanuel’s hurricane model and potential 881  
839 intensity theory. *Quart. Journ. Roy. Meteor. Soc.*, **134**, 882  
840 551–561.

841 Smith, R. K., M. T. Montgomery, and S. Wang, 2025: Can 883  
842 one reconcile the classical theories and the WISHE- 884  
843 theories of tropical cyclone intensification? *Tropical 885  
844 Cyclone Research and Review*, **14**, 105–118.

845 Smith, R. K., C. W. Schmidt, and M. T. Montgomery, 2011: 846  
846 Dynamical constraints on the intensity and size 847  
847 of tropical cyclones. *Quart. Journ. Roy. Meteor. Soc.*, 848  
848 **137**, 1841–1855.

849 Smith, R. K., and G. L. Thomsen, 2010: Dependence of 850  
850 tropical-cyclone intensification on the boundary layer 851  
851 representation in a numerical model. *Quart. Journ. 852  
852 Roy. Meteor. Soc.*, **136**, 1671–1685.

853 Smith, R. K., and S. Vogl, 2008: A simple model of the 854  
854 hurricane boundary layer revisited. *Quart. Journ. Roy. 855  
855 Meteor. Soc.*, **134**, 337–351.

856 Smith, R. K., and S. Wang, 2018: Axisymmetric balance 857  
857 dynamics of tropical cyclone intensification: Diabatic 858  
858 heating versus surface friction. *Quart. Journ. Roy. 859  
859 Meteor. Soc.*, **144**, 2350–2357.

860 Sobel, A., S. Camargo, and M. Previdi, 2019: Aerosol 861  
861 versus greenhouse gas effects on tropical cyclone 862  
862 potential intensity and the hydrologic cycle. *J. Climate*, 863  
863 **32**, 5511–5527.

864 Tang, B., and K. A. Emanuel, 2010: Midlevel ventila- 865  
865 tion’s constraint on tropical cyclone intensity. *J. Atmos. 866  
866 Sci.*, **67**, 1817–1830.

867 Turner, J. S., and D. K. Lilly, 1963: The carbonated-water 868  
868 tornado vortex. *Quart. Journ. Roy. Meteor. Soc.*, **20**, 869  
869 468–471.

870 Vinour, L., and M. T. Montgomery, 2026: Improved 871  
871 understanding of the tropical cyclone lifecycle in real- 872  
872 istic simulations through the perspective of eyewall 873  
873 ventilation and boundary layer mass flux. *Tropical 874  
874 Cyclone Research and Review*, **15**, in press.

875 Zhang, D.-L., Y. Liu, and M. K. Yau, 2001: A multi-scale 876  
876 numerical study of Hurricane Andrew (1992). Part IV: 877  
877 Unbalanced flows. *Mon. Wea. Rev.*, **61**, 92–107.

878 Zhang, J. A., 2010: Estimation of dissipative heating 879  
879 using low-level in situ aircraft observations in the 880  
880 hurricane boundary layer. *J. Atmos. Sci.*, **67**, 1853– 881  
881 1862.

882 Zhang, J. A., and M. T. Montgomery, 2012: Observa- 883  
883 tional estimates of the horizontal eddy diffusivity and 884  
884 mixing length in the low-level region of intense hurri- 885  
885 canes. *J. Atmos. Sci.*, **69**, 1306–1316.